Int J Biometeorol (2002) 46:9–21
DOI 10.1007/s004840100105

ORIGINAL ARTICLE

Paolo Manunta · Robert F. Grant · Yongshen Feng
Bruce A. Kimball · Paul J. Pinter
Robert L.A. La Morte · Douglas J. Hunsaker
D.J. Wall

Changes in mass and energy transfer between the canopy and the atmosphere: model development and testing with a free-air CO_2 enrichment (FACE) experiment

Received: 25 October 2000 / Accepted: 16 July 2001 / Published online: 16 November 2001

Abstract The rationale for this study is found in the probable higher temperatures and changes in rainfall patterns that are expected in the future as a result of increasing levels of CO_2 in the atmosphere. In particular, higher air temperatures may cause an increase in evapotranspiration demand while a reduction in rainfall could increase the severity and duration of drought in arid and semi-arid regions. Representation of the water transfer scheme includes water uptake by roots and the interaction between evapotranspiration and CO_2 enrichment. The predicted response of a spring wheat (*Triticum aestivum* L. cv. Yecora rojo) canopy in terms of energy exchange processes to elevated atmospheric CO_2 level was tested against measurements collected at the FACE (Free Air Enrichment Experiment) site in 1994. Simulated and measured canopy conductances were reduced by about 30% under elevated [CO_2] under optimum conditions of water supply. Reductions in latent heat fluxes under elevated instead of ambient [CO_2] caused reductions in both simulated and measured seasonal water use of 6% under optimum and 2% under suboptimum irrigation. The soil–plant–atmosphere water transfer scheme proposed here offers several advances in the simulation of land surface interactions. First, the stomatal resistance model minimizes assumptions in existing land surface schemes about the effects of interactions among environmental conditions (radiation, temperature, CO_2) upon stomatal behavior. These interactions are resolved in the calculation of CO_2 in which processes are already well understood.

P. Manunta (✉) · R.F. Grant · Y. Feng
Department of Renewable Resources, University of Alberta, AB T6G 2E3, Canada
e-mail: paolo.manunta@gov.ab.ca

B.A. Kimball · P.J. Pinter · R.L.A. La Morte · D.J. Hunsaker
D.J. Wall
U.S. Water Conservation Lab, USDA-ARS, Phoenix, AZ 85040, USA

Keywords Modelling · Climate change · Elevated CO_2 · Energy balance · wheat

Introduction

There is growing realization that terrestrial ecosystems are dynamically linked to global climate. An improved representation of these ecosystems must be included in models used to predict how climate will respond to human perturbation. During the last decade a wide variety of ecosystem models have been used to represent terrestrial processes. Three classes of these models have emerged (Foley 1995): (1) terrestrial biogeochemical models (2) potential vegetation models and (3) soil–vegetation–atmosphere transfer (SVAT) models. In some instances the use of these models has been extended to the investigation of global vegetation patterns as affected by different predicted climatic scenarios (Prentice et al. 1992).

Surface hydrology (sensible and latent heat transfer, runoff) has been indicated as a key component of SVAT (Garratt 1993). Canopy stomatal conductance is important in SVAT models because it affects energy and mass exchange between terrestrial ecosystems and the atmosphere. Stomatal conductance depends upon several interacting environmental conditions such as physiological conditions of the plant, soil water availability, intensity of short-wave radiation, air humidity, leaf temperature, and [CO_2] (Steward 1988; Jones and Higgs l989). A technique for calculating canopy stomatal conductance proposed by Jarvis (1976) uses an unconstrained value for conductance multiplied by a series of dimensionless factors representing constraints imposed by each environmental condition known to affect conductance. However, it is difficult to determine the unconstrained conductance for different plant species and the extent to which this conductance is reduced by different combinations of environmental conditions.

Such a non-mechanistic representation of stomatal conductance may cause inaccuracies in the simulation of latent and sensible heat transfer. Although a truly mechanistic model is most likely to be successful in predicting stomatal responses, its implementation is not always feasible because parameters such as maximum stomatal conductance or the sensitivity to leaf vapor pressure deficit need to be readjusted to fit a particular vegetation type. The approach used in this paper expands upon the analysis of Ball (1988) and the experimental findings of Wong et al. (1979), which suggest an implicit dependence of stomatal conductance on photosynthesis, and therefore the role of stomatal conductance in regulating the balance between transpiration and net uptake of CO_2 during photosynthesis (Collatz et al. 1991). Although some of the components of this model, particularly CO_2 fixation, are based on fundamental properties of the plant biochemical processes, this approach remains largely empirical. The first step of this work was to separate the response of stomatal conductance to changes in those environmental variables that have an effect on photosynthesis from the response to those that do not. For example, changes in incoming photosynthetic photon flux density are likely to cause a proportional change in stomatal conductance so as to maintain a constant proportionality between stomatal conductance and photosynthesis, if all other factors are held constant. By contrast, changes in leaf water potential cause a direct change in stomatal conductance (Cline and Campbell 1976). It could be argued that opening and closing of the pore is turgor-dependent (Raschke 1979), however, the ion transport processes and the sensory system that control the closing are not fully understood.

New insights into the biochemical mechanisms governing stomatal conductance were provided by plant physiologists in the 1980s and early 1990s (Farquhar et al. 1980; Ball 1988; Collatz et al. 1991) and are being used in SVAT models (Foley et al. 1996; Sellers et al. 1996) coupled with atmospheric general circulation models Wong et al. (1979) concluded that stomatal conductance is determined by the CO_2 fixation rate of the mesophyll. When they applied inhibitor of photosynthetic electron transport or abscisic acid, changes in the stomatal conductance were proportional to those in the CO_2 fixation rate. A mesophyll signal that governs stomatal aperture is plausible, but mechanistic evidence in support of this hypothesis is still missing. It has been argued that a system regulating stomatal functioning must activate a compromise between providing CO_2 for assimilation and restricting water loss (Raschke 1979).

Two processes that are expected to be affected by higher $[CO_2]$ in the atmosphere are assimilation and conductance to water vapor. Previous studies report that when $[CO_2]$ was raised from the ambient level to 530 μmol mol^{-1} the photosynthetic rate of wheat increased by about 12% (Sicher and Bunce 1997). Other authors reported an increase of about 50% when $[CO_2]$ was elevated from the ambient level to about 600 μmol mol^{-1} under light-saturated conditions (Miglietta et al. 1996). Although the absolute increase could be affected by plant nutrition status and perhaps by acclimation, Guehl et al. (1994) reported that higher $[CO_2]$ produces a higher biomass accumulation. Although reduced stomatal conductance to water vapor leads to a decrease in transpiration (Kimball and Idso 1983; Senock et al. 1996), the extent of this decrease is a balance between the higher CO_2 fixation and the reduced stomatal aperture induced by higher $[CO_2]$. However, the higher amount of CO_2 may result in a higher leaf-area index, therefore the overall reduction in transpiration found at the leaf level may not be retained when the overall canopy transpiration is considered.

Water stress reduces stomatal conductance by decreasing soil and plant water potentials and by inhibiting mesophyll carbon fixation (Chaves 1991). Foley et al. (1996) represented heuristically the effect of water stress on fixation by calculating a stress factor based on plant available water. We recognize that this representation is justified by uncertainties about the extent to which water stress causes stomatal closure or inhibits fixation capacity. However, we propose an alternative approach that is easier to test with field measurements. This approach involves the calculation of leaf water potential, which is then used in the stomatal model to reduce conductance and consequently fixation rate. The leaf water potential is calculated by accounting for the balance between plant water content plus plant water uptake and transpiration. This calculation takes also into account the amount of water stored in the plant tissue. Plant water uptake is a function of root and soil properties that together constitute a series of resistances to water flow from the soil through the plant.

We present here a formulation of canopy stomatal conductance that could be used in SVAT models, which is based on the biochemical mechanisms described above as represented by Ball (1988). This formulation is extended to include the effects of plant water potential on stomatal conductance as proposed above, and it includes explicit calculations of plant CO_2 fixation, respiration and both above- and below-ground productivity as affected by soil and atmospheric conditions. The purpose of this formulation is to provide estimates of latent and sensible heat, as well as of net carbon assimilation rates, from which ecosystem productivity may be calculated. These estimates are compared with diurnal energy fluxes, and with seasonal water use and the phytomass of a wheat crop exposed to ambient as opposed to elevated CO_2 (355 versus 550 μmol mol^{-1}), and to optimum as opposed to optimum irrigation as part of free-air CO_2 enrichment (FACE) experiment. Assessing the accuracy of this simulation is crucial in determining our level of confidence in estimates of the mass and energy exchange between vegetation and the atmosphere, provided by land-surface models to global circulation models used in climate change or water balance studies.

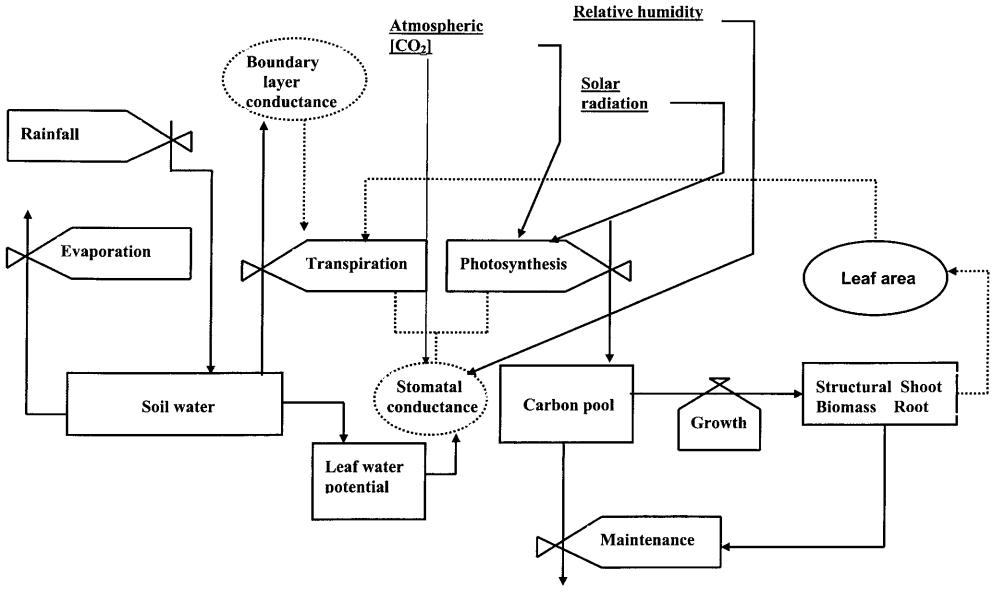

Fig. 1 Relational diagram of the essential components of gas exchange between the canopy and the atmosphere where water shortage is a controlling factor. *Rectangles* state variables, *valve symbol* rates, *circles* auxiliary variables, *underlined variables* external variables. *Solid lines* flows of material, *broken lines* flow of information

Materials and methods

Model development

The approach used in the model development was aimed at easier testing with field data such as energy balance, leaf level photosynthesis, conductance and water potential. Calculation of the canopy water potential is used in the stomatal formulation to eventually reduce conductance and CO_2 fixation rate. Leaf water potential is used to represent the canopy water status as affected by transpiration and available soil water. The leaf water potential is calculated by accounting for the changes in plant water content that result from the balance between plant water uptake and transpiration. The water capacitance of the plant tissue is also used in the calculation of the changes in plant water content. Plant water uptake is a function of root and soil properties that together constitute a series of resistances to water flow from the soil through the plant. The overall structure of the model is summarized in the form of a relational diagram (Fig. 1). Although, in this arid environment, crop production relies almost exclusively upon dripping irrigation, the model accounts for the evaporation of canopy-intercepted rainfall that may occur.

The plant component, including the stomatal conductance, photosynthesis and plant growth have been integrated with the formulation of the energy balance described in detail by Verseghy et al. (1993). The plant and soil water balance is computed by coupling the exchange of mass and energy between the canopy and the atmosphere to the three soil layers (Verseghy 1991). Further details regarding the formulation of the energy balance equation, including the approach used to account for partial canopy cover, can be found in Verseghy et al. (1993). The work reported here has the implicit advantage of using calculated values of soil water content and energy balance that otherwise would have to be provided as a direct input to the plant model as done in previous studies (Williams et al. 1993).

Relations between water and the plant

The exchange of water vapor between the canopy and the atmosphere makes use of a modified version of stomatal formulation proposed by Ball (1988). This model is used to calculate the value of the conductance (g_s, mol m^{-2} S^{-1}) for two classes of leaves, sunlit and shaded respectively.

$$g_s = \left(m\frac{A_n}{C_a} + b\right)\frac{1}{\left[1+\left(\frac{\Psi_l}{\Psi_c}\right)^n\right]} \quad (1)$$

Conductance is driven by CO_2 uptake (A_n, μmol m^{-2} s^{-1}) and reduced by increasing atmospheric [CO_2] (C_a, μmol mol^{-1}). The terms *m* and *b* in Eq. 1 are the slope and intercept parameters obtained independently from linear regression analysis of leaf level measurements by Ball (1988) and Collatz et al. (1991). Plant water status is expressed as the ratio between Ψ_l leaf water potential (MPa) and Ψ_c the critical water potential at which stomatal conductance becomes half of the maximum value observed (Campbell 1985). Then value is a slope factor that expresses the increase in resistance as a function of the leaf water potential. Relations of this type have been reported by several authors (e.g. Cline et al. 1976; Glatze1 1983). This value for *n* can be as low as 3 or as high as 20 depending upon species (Campbell 1985). For reason of convenience the conductance is converted into cm s^{-1}, a conductance of 1 cm s^{-1} being approximately 0.4 mol m^{-2} s^{-1} at 25 °C and an atmospheric pressure *P*=101.3 kPa. Conductance to water vapor expressed in cm s^{-1} is then converted into resistance expressed in m s^{-1}.

The value of A_n, in Eq. 1 is modelled as the minimum of the dark (J_c) and light (J_e) reaction rates in CO_2 fixation (μmol m^{-2} s^{-1}):

$$A_n \approx \min(J_c J_e) \quad (2)$$

The dark reaction rate is calculated for conditions of saturating irradiance and competitive inhibition by oxygen according to the following formulation (Farquhar et al. 1980):

$$J_C = \frac{V_{cmax}\left([C_l] - \Gamma^*\right)}{[C_l] + k_c\left(1 + \frac{[O_l]}{k_o}\right)} \quad (3)$$

The maximum dark reaction rate (V_{cmax}, μmol m^{-2} s^{-1}) is assumed to be at ambient temperature and saturating CO_2 in the absence of oxygen. The variables [C_i] and [O_i] represent the liquid concentrations (μM) of CO_2 and O_2 in the stroma, Γ^* is the compensation point for gross photosynthesis (μM) at the current level of CO_2 and O_2, k_c and k_o are the Michaelis-Menten constants (μM) for CO_2 and O_2 (Douglas and Ogren 1984). The value of V_{cmax} is derived from a standard value obtained at 30°C (Grant 1989) and adjusted for temperature according to Sharpe and DeMichelle (1977) using parameters from Farquhar et al. (l980). Intercellular CO_2 ([C_i], μM) and O_2 ([O_i], μM) concentrations are obtained from the intercellular concentration of CO_2 and O_2 (μmol mol^{-1}) using a

temperature-dependent solubility function (Wilhelm et a1. 1977) assuming that mesophyll resistance to CO_2 is negligible. Intercellular CO_2 concentrations for C_3, and C_4 plants are set to be a fraction of the atmospheric concentration (0.7 and 0.5 respectively). The compensation point for gross photosynthesis Γ^* in Eq. 3 (μM) at current levels of CO_2 and O_2 is calculated as:

$$\Gamma^* = \frac{0.5 V_{\mathrm{omax}} k_{\mathrm{c}} O_{\mathrm{l}}}{V_{\mathrm{cmax}} k_{\mathrm{o}}} \tag{4}$$

where V_{cmax} (in μmol m^{-2} s^{-1}) represents the maximum rate of oxygenation under conditions of saturating O_2 and in the absence of CO_2 and is assumed to be 0.21 V_{cmax} (Farquhar et al. 1980). As in the case for maximum capacity of Rubisco, the maximum oxygenation rate V_{cmax} at ambient temperature is derived from a standard value obtained at 30°C and adjusted for temperature according to Sharpe and DeMichelle (1977) using parameters from Farquhar et al. (1980).

The light reaction rate of photosynthesis is given by:

$$J_{\mathrm{e}} = JQ \tag{5}$$

where Q, is the ratio of CO_2 fixation to electron transport (mol mol^{-1}), which is estimated as:

$$Q = \frac{C_{\mathrm{i}} - \Gamma^*}{e^- C_{\mathrm{l}} + 10.5\Gamma^*} \tag{6}$$

(Farquhar and von Caemmerer l982) The term e^- is the electron requirements for CO_2 fixation. This value is set to be equal to 4.5 and to 7.5 for C_3 and C_4 plants respectively. The potential electron transport rate J (μmol m^{-2} s^{-1}) in Eq. 5 is obtained from:

$$J = \frac{\alpha I + J_{\max} - \left[(\alpha I + J_{\max})^2 - 4\theta\alpha I J_{\max}\right]^{0.5}}{2\theta} \tag{7}$$

(Evans and Farqhuar l991) where α = quantum efficiency (0.5 mol electrons mol $quanta^{-1}$), I is the absorbed photosynthetically active radiation (μmol quanta m^{-2} s^{-1}), and J_{max} is the maximum rate of electron transport (μmol electrons m^{-2} s^{-1}) adjusted for temperature according to Farquhar et al. (1980). The value for J_{max} was derived from measurements on spinach plants (*Spinacia oleacia* L.) and reported in Evans and Farquhar (l991). The curvature factor θ ranges from 0 to 1 and represents the transition of J from the region of maximum quantum yield to the light saturated rate. The region where quantum yield is maximized is found at low irradiance level, where the relation between J and I is most linear.

The value of I is calculated as a spatially averaged value for each of two leaf classes, sunlit and shaded. The sunlit class intercepts the direct solar beam plus diffuse sky radiation and the shaded class receives only diffuse sky radiation. This approach represents the non-linear response of leaf level physiological processes to different intensities of solar radiation within the canopy (Forseth and Norman 1993; Norman 1993). Because the actual fraction of sunlit and shaded leaves changes with time of the day, the absorption coefficient representing random leaf inclination and orientation is corrected for the sine of the solar elevation angle.

The assimilation rate A_n of each leaf class (Eqs. 2 –7) is used to calculate its stomatal conductance unconstrained by water availability (Eq. l with, Ψ_l =0 MPa). This conductance is multiplied by the leaf area of each class, and the products of both classes are added to estimate unconstrained canopy stomatal conductance. Although temperature, humidity and wind speed might differ for different positions inside complex canopies this scaling technique does not specifically account for these variations.

Leaf water potential is calculated by coupling canopy transpiration T to soil water uptake U_z, calculated as the sum of that from each soil layer l, and where z is the number of soil layers:

$$T = \sum_{z=1}^{l} U_z \sum_{z=1}^{l} \frac{(\Psi_{\mathrm{l}} - \Psi_{\mathrm{sz}})}{(r_{\mathrm{rz}} + r_{\mathrm{sz}})} \tag{8}$$

Root resistance to water uptake r_{rz} is related to the amount of roots present in each layer (Campbell 1985):

$$r_{\mathrm{rz}} = \frac{\rho_{\mathrm{r}}}{L_z \Delta z} \tag{9}$$

where ρ_r is root radial resistivity (s m^{-1}), L_z is the root length density (m m^{-3}) and Δz is the depth increment (0.10, 0.25, and 3.75 m) of the three soil layers. Radial water flow from the soil to the roots is represented as that through a hollow cylinder (Gardner l960; Cowan 1965). Passioura and Cowan (1968) solved numerically the non-linear equation of radial flow to the root and found that a more exact result is obtained under the assumption of "steady-rate" rather than "steady-state" flow as previously suggested by Gardner (l960). The following equation is used then to approximate radial flow resistance under steady-rate conditions:

$$r_{\mathrm{sz}} = \ln\left(\frac{b_z}{2.1a}\right) / (2\pi K_z L_z \Delta z) \tag{10}$$

where a is the radius of the root (m), K_z, is the soil hydraulic conductivity (m s^{-1}) and b_z is the path length for water uptake (m) obtained as:

$$b_z = (\pi L_z)^{-0.5} \tag{11}$$

Conductance to water vapor decreases as Ψ_l drops, Eq. (1), while water uptake varies positively with a decreasing Ψ_l due to the effect of Ψ_l upon the gradient between Ψ_l and Ψ_{sz} in Eq. (8). The resulting water uptake is inversely related to the sum of the root r_{rz} and soil r_{sz} resistance. Outward (transpiration) and inward (uptake) fluxes are mediated in part by the leaf water potential, there is therefore an equilibrium value for Ψ_l, under any combination of soil and atmospheric conditions at which transpiration equals uptake. This value is calculated through an iterating procedure, thereby a value for Ψ_l is found at which transpiration from the energy balance is equilibrated with total water uptake from Eqs. 8 –11. After the initial leaf water potential is computed, the difference between the transpiration and the water uptake by the roots and the water stored in the canopy is calculated. When the difference is less than 0 the calculated water uptake by the roots is too large, therefore the gradient between plant and soil is too steep, consequently the leaf water potential is lowered. If, on the other hand, the difference is more than 0 the water uptake by roots is too small, therefore the gradient between plant and soil is too low, consequently the leaf water potential is increased. The process continues until the difference is close to 0, then the iteration stops and the 1eaf water potential calculated is used to represent the plant water status (Grant et al. 1999). When the stomatal conductance is reduced because of leaf water potential, the CO_2 fixation is also proportionally reduced while the internal [CO_2] is preserved. Therefore the reduction in CO_2 fixation via reduction in stomatal conductance preserves the formulation proposed by Ball (1987), in which the assimilation rate is the result of conductance times the difference between the atmospheric and internal [CO_2].

Plant carbon balance and vegetation dynamics

Products of CO_2 fixation (A_n from Eqs. 2 –7) are accumulated in a storage pool from which C is partitioned among leaves, stems and roots as a function of accumulated degree days (van Keulen and Seligman 1987), and from which C is respired according to maintenance and growth requirements for energy (Amthor 1984). The maintenance requirement is calculated by multiplying the phytomass of leaves, stems and roots by organ maintenance coefficients (g C g C^{-1} h^{-1}) and by a temperature function with a Q_{10} of 2 (McCree 1988). The growth requirement is calculated from organ growth yields (McCree 1988) and is removed from storage C after the maintenance requirement has been removed. Growth in leaf and root phytomass is converted into growth in leaf area and root length according to a function for specific leaf area and specific root length. Leaf areas and root lengths are used to calculate irradiance interception and water uptake as described above. Finally, plant senescence is controlled by the accumulation of heat units.

Field experiment

Spring wheat *(Triticum aestivum* L. cv. Yecora rojo) was planted at a density of 180 plants m^{-2} on 8 December 1993 in a 4-ha field of Trix clay loam (calcareous) soil (Kimball et al. 1992a) at the Maricopa Research Center 30 km from Phoenix, Ariz. (Latitude 33.04°, longitude −111.58°). Shortly after planting, two 25-m-diameter rings were placed in each of four replicates near the center of the field. Each replicate was divided into strips, one receiving high irrigation and one receiving low irrigation. The rings were constructed to emit CO_2 through holes in a series of vertical pipes 5 m in height connected to the ring every 2.0 m. Inside the ring there were two plots, one receiving high irrigation and one receiving low irrigation amounts. An average $[CO_2]$ of 550 μmol mol^{-1} was maintained over one of the rings in each replicate by blowing CO_2 -enriched air from upwind emitters (Lewin et al. 1994). A $[CO_2]$ close to the ambient value (355 μmol mol^{-1}) was maintained over the other rings. Irrigation treatments, including an optimum treatment in which evapotranspirational demand was fully replaced and a sub-optimum treatment in which half of the demand was replaced, were applied to one half of every ring using a subsurface drip system. The experimental area was located within the boundaries of an irrigation district so that the CO_2 -enriched (FACE) and the control treatments were surrounded by more than 1 km irrigated fields in all directions.

During the entire experiment, hourly averaged values were recorded for solar radiation, air temperature, wind speed, humidity, and precipitation. Phytomass was measured weekly from approximately 24 plants collected in each treatment replicate (Pinter et al. 1996). Soil moisture measurements were made twice a week with neutron probes at 0.20-m intervals to a depth of 2.1 m. A portable gas analyzer (model 6200, Li-cor Inc., Lincoln, Neb. USA) was used to measure leaf stomatal conductance and photosynthesis from three or four recently expanded sunlit leaves in each replicate. Owing to the relatively short and simple canopy found in the field, we directed our efforts toward the sampling of only sunlit leaves. However, the overall mass and energy transfer of a complex and tall canopy should have a more sophisticated model representation and testing for shaded leaves. The sampling took place between sunrise to sunset at stem extension (22 March the 81st day of the year) and anthesis (5 April, day 95).

During the experiment, net radiation was measured with net radiometers (model Q6, Radiation and Energy Balance Systems, Seattle, wash., USA) mounted 0.4 m above the canopy. Soil heat-flux estimates were obtained using four heat-flux plates per plot (model HFT-3, Radiation and Energy Balance Systems, Seattle, wash., USA) placed 0.10 m deep, and thermocouples 0.05 m above the plates to measure the heat stored in that portion of soil. The air temperature was measured with a pair of customized aspirated psychrometers placed at 2 m in each plot. Canopy temperature was measured with a set of two stationary infrared thermometers (model 4000a, 15°field of view, Everest Interscience, Tustin, calif.) in each plot (Kimball et al. 1995). Prior to installation in the field, the infrared thermometers were calibrated over a wide range of temperatures, using a black-body source (model 250, Advanced Kinetics, Huntington Beach, calif., USA). Aerodynamic resistance was calculated from wind speed at 2 m measured with a cup anemometer (mode1 12102D, R.M. Young Co., Traverse City, Mich., USA), and from zero-plane displacement, roughness length, and a non-isothermal stability correction (Mahrt and Ek 1984). These measurements were used to calculate sensible heat flux, and latent heat flux was estimated as the residual term in the surface energy balance. Limitations in instrumentation allowed these measurements to be taken only on the optimally irrigated plots.

Simulation experiment

In the model the soil hydraulic properties are derived from tabulated values grouped in 11 soil textural classes (Cla Homberger l978). Soil texture data recorded at the site (Kimball et al. 1992a)

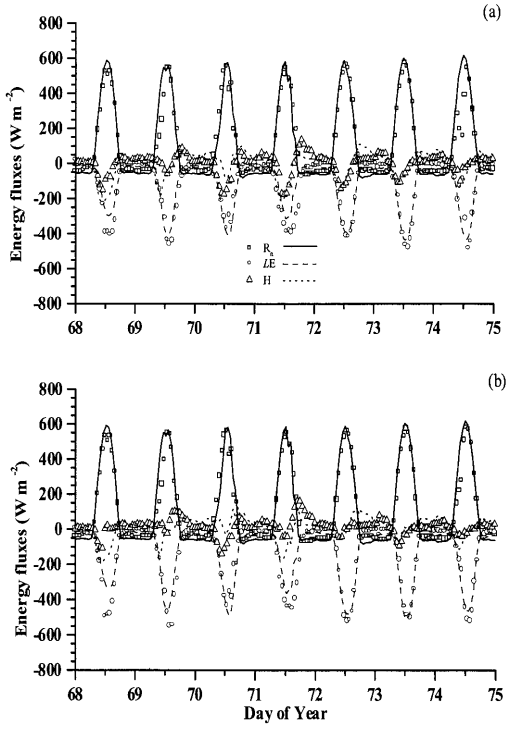

Fig. 2 Net radiation (R_n), sensible heat (H) and latent heat (LE) fluxes simulated (*lines*) and measured (*symbols*) under (**a**) 550 and (**b**) 355 μmol mol^{-1} CO_2 and optimum water supply from 10 to 16 March 1994 (days of year: 69–75)

Table 1 Plant biological parameters used in simulation. The number in parantheses indicates the equation in the text in which the parameters are used

Parameter	Value for C_3 (broadleaf)
Photosynthesis formulation	
V_{cmax} (3, 4)	90 μmol m^{-2} s^{-1} at 30 °C
k_c (3, 4)	12.5 μM
k_0 (4, 5)	500 μM
e^- (6)	4.5 mol e^- mol CO_1 $^{-1}$
α (7)	0.5 mol e^- mol $quanta^{-1}$
J_{max} (7)	180 μmol e^- m^{-2} s^{-1}
θ (7)	0.8
Stomatal conductance formulation	
m (1)	6.0
b (1)	0.020 mol m^{-2} s^{-1}
Ψ_c (1)	0.2 MPa
n (1)	10

were used in the model, together with the biological properties of the plant functional type (C_3) (Table 1) and the atmospheric $[CO_2]$ (μmol mol^{-1}).

Although a subsurface irrigation system was used in the field, the model does not allow subsurface water additions, so that irrigation was delivered during the simulation in the form of nighttime rainfall events. Transport of sensible heat and water vapor through the canopy was proportional to aerodynamic conductance calculated according to Van Bavel and Hillel (1976). To prevent erroneous values in the calculation of the aerodynamic resistance caused by extremely low wind speed found at the experiment location, the Richardson number was constrained between –0.10 and 0.05. In order to minimize modelled losses due to evapora-

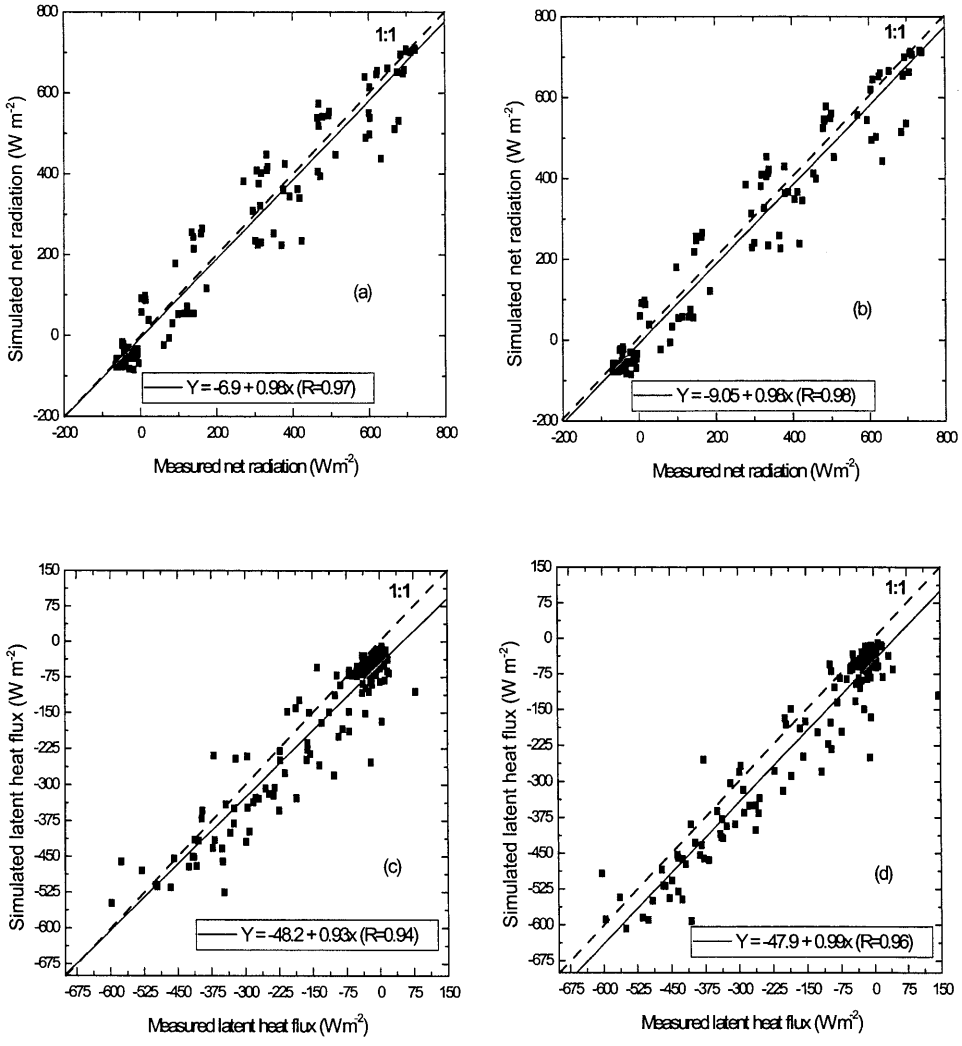

Fig. 3 Correlation between measured and simulated parameters: net radiation (**a**), latent heat flux (**c**) under 550 μmol mol^{-1} CO_2; net radiation (**b**), latent heat flux (**d**) under 355 μmol mol^{-1} CO_2 both with optimum water supply from 24 to 30 April 1994 (days 114–120)

tion, subsurface irrigation was added as rain occurring at night. Model outputs for energy balance, canopy temperature, leaf conductance and phytomass growth were compared with those measured in the field experiment under ambient as opposed to elevated CO_2.

Results

Modelled and measured results were compared over two representative weeks (10–16 March, days of the year 69–75, and 24–30 April, days 114–120) of the FACE experiment (Figs. 2, 3). Average values for solar radiation, air temperature and vapor density during the first week were 243 W m^{-2}, 15.7 °C and 6.6 g m^{-3}; and those during the second week were 297 W m^{-2}, 15.7 °C and 5.7 g m^{-3}. Latent heat fluxes were understimated by 50–100 W m^{-2} during the first week of comparison (10 and 13 March; days 69 and 72) but were otherwise within 50 W m^{-2} (2 × SE of the measured fluxes) under both 355 and 550 μmol mol^{-1} CO_2 with optimum irrigation (Fig. 2a, b).

During the second week of comparison in April, simulated net radiation 4 and simulated latent heat fluxes were linearly correlated with the measured values under 355 μmol mol^{-1} CO_2 (Fig, 3a, c) and under 550 μmol mol^{-1} CO_2 (Fig. 3b, d). Both these treatments under optimum irrigation had a correlation coefficient between 0.94 and 0.98. However simulated sensible heat flux correlated less strongly with the measured field values for both CO_2 treatments (Fig. 4a, b). The lowest correlation coefficients (0.71 and 0.66 respectively) were calculated between simulated and measured changes in latent and sensible owing heat to reduction in transpiration caused by the CO_2 enrichment (Fig. 4c, d).

With optimum irrigation in March both simulated and measured latent heat fluxes were lower under 550 than under 355 μmol mol^{-1} CO_2 by amounts that varied diurnally from 0 W m^{-2} during the nights to about 50 W m^{-2} during the afternoons. With optimum irrigation in April, both simulated and measured latent heat fluxes were lower under 550 than under 355 μmol mol^{-1} CO_2 by amounts that varied diurnally from 0 W m^{-2} during the nights to between 50 and 100 W m^{-3} during the afternoons early in the week.

Diurnal changes in simulated plant water relations, including leaf water potential, temperature, sunlit leaf

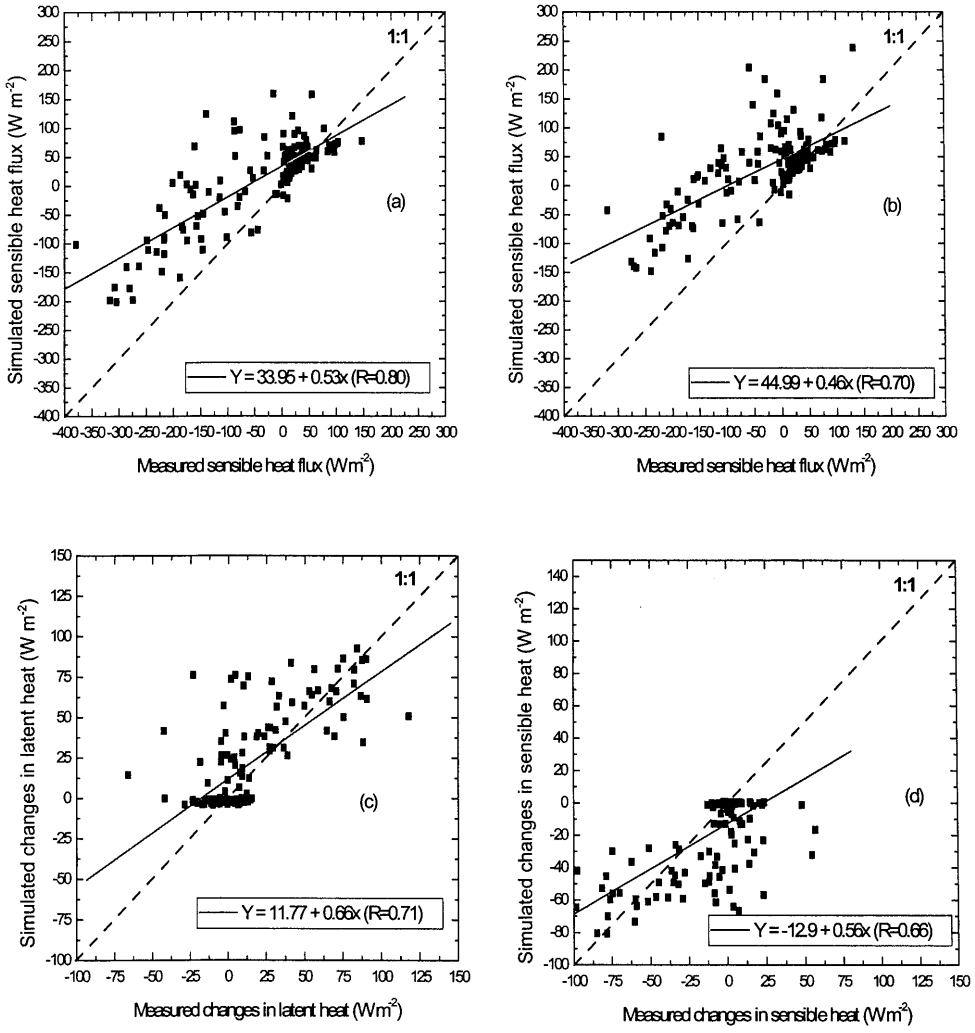

Fig. 4 Correlation between measured and simulated parameters: sensible heat flux (**a**), changes in latent heat flux (**c**) under 550 μmol mol^{-1} CO_2; sensible heat flux (**b**), changes in latent heat flux (**d**) under 355 μmol mol^{-1} CO_2 both with optimum water supply from 24 to 30 April 1994 (days 114–120)

conductance and photosynthesis, were compared with measured values during two selected days: 22 March (81st day of the year) and 5 April (day 95). On 22 March the optimum irrigation plots had last been irrigated 1 day earlier, and the suboptimum irrigation plots 6 days earlier, so that the simulated canopy water potential remained comparatively high (Fig. 5a). Under elevated [CO_2], midday values of the simulated and measured leaf water potential increased by 0.1 and 0.24 ± 0.13 MPa with optimum irrigation, and by 0.05 and 0.14 ± 0.25 MPa under suboptimum irrigation. Because both treatments had been irrigated 6 days before, the simulated and measured conductances were only slightly lower under suboptimum than under optimum irrigation (Fig. 5b). Comparison of simulated with measured values was complicated by the large variability in the latter. Midday values of simulated stomatal conductances were reduced relatively more under 550 μmol mol^{-1} CO_2 with optimum, than with suboptimum irrigation (to 0.72 composed to 0.86 of conductances under 355 μmol mol^{1} CO_2). The measured conductances were affected likewise (to 0.57 ± 0.21 compared to 0.68 ± 0.14 of conductances under 355 μmol mol^{-1} CO_2). Irrigation applied 6 days before caused both simulated and measured canopy temperatures to be only 1.5–2.0 °C higher under suboptimum than under optimum irrigation (Fig. 5c). Reduced conductance under 550 μmol mol^{-1} CO_2 caused simulated midafternoon canopy temperatures to increase by 0.9 °C and 0.5 °C under optimum and suboptimum irrigation respectively. These increases, were slightly less than those of 1.5 °C and 1.0 °C measured with the mobile infrared thermometers. The conductance simulated on 22 March (Fig. 5b) allowed high carbon fixation rates even under suboptimum irrigation (Fig. 5d). Simulated CO_2 fixation was generally lower than the measured values, owing to the spatial averaging of irradiance intensity on the sunlit leaf surface in the model. Simulated carbon fixation was increased relatively more under 550 mol mol^{-1} CO_2 with suboptimum than with optimum irrigation (to 1.33 compared to 1.12 of values under 355 mol mol^{-1} CO_2). The measured rates were affected likewise (to 1.26 ± 0.18 compared to 1.20 ± 0.13 of values under 355 μmol mol^{-1} CO_2).

On 5 April, the high-irrigation plots had last been irrigated 1 day earlier, and the low irrigation plots 8 days earlier. Simulated leaf water potentials for all the treat-

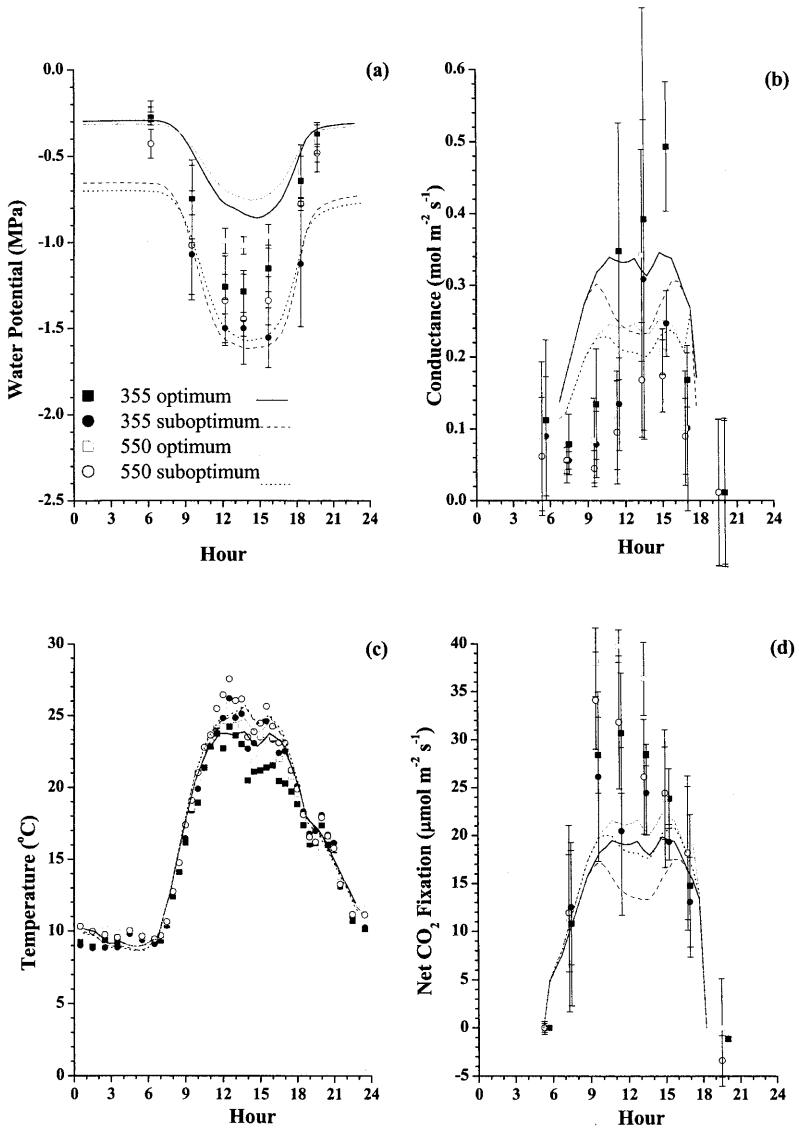

Fig. 5 (**a**) Leaf water potential, (**b**) leaf stomatal conductance, (**c**) canopy temperature and (**d**) leaf net CO_2 fixation simulated (*lines*) and measured (*symbols*) under optimum or suboptimum water supply and 550 or 355 μmol mol^{-1} CO_2 on 22 March 1994 (day 81)

Table 2 Evapotranspiration and phytomass measured (*M*) and simulated (*S*) under 355 and 550 μmol mol^{-1} CO_2 and suboptimum and optimum irrigation

Parameter	Irrigation	355 μmol mol^{-1} CO_2 (*A*)		550 μmol mol^{-1} CO_2 (*B*)		B–A (%)	
		M	S	M	S	M	S
Phytomass (g m^{-2})	Suboptimum	1,361 ± 97	1176	1,604 ± 151	1,505	+18%	+28%
	Optimum	1,856 ± 145	2279	2,044 ± 167	2,589	+10%	+14%
Evapotranspiration (mm)	Suboptimum	476 ± 27	478	465 ± 15	470	–2.3%	–1.7%
	Optimum	751 ± 10	757	710 ± 17	711	–6.6%	–6.6%

ments (i.e., CO_2 × irrigation) were correlated with the measured field values (Fig. 6a). Similarly, simulated leaf conductance (Fig. 6b), canopy temperature (Fig. 6c), and CO_2 fixation rates (Fig. 6d) were also correlated with measured field values. The more robust correlation (r = 0.99) was obtained for the canopy temperature; leaf water potential and leaf conductance had correlation coefficients of 0.77 and 0.75 respectively. The lowest correlation coefficient (r = 0.60) was obtained between simulated and measured net CO_2 fixation rates.

The time-integrated effects of CO_2 and irrigation on mass and energy exchange can be seen in the growth and water use of above-ground phytomass. The seasonal time course of leaf area index was simulated within the

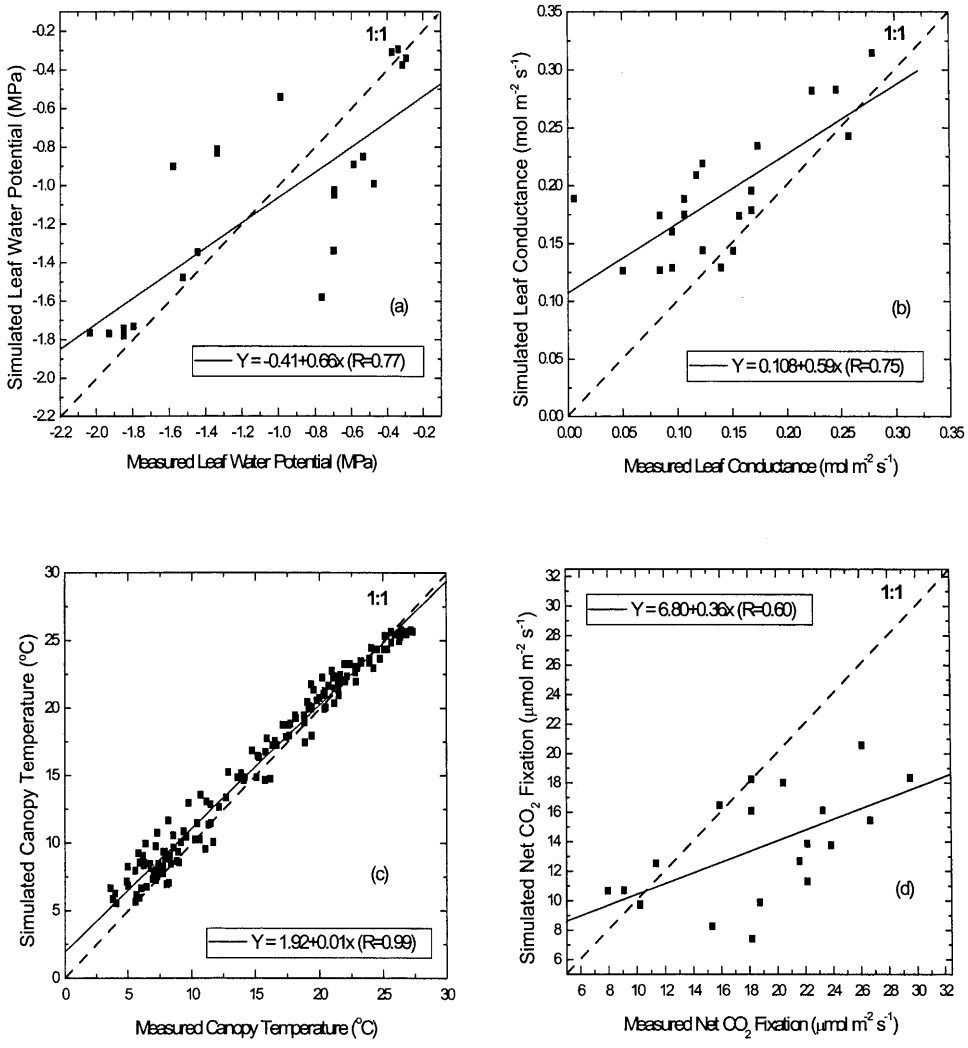

Fig. 6 Correlation between measured and simulated parameters: leaf water potential (**a**), leaf stomatal condectance (**b**) canopy temperature (**c**), leaf net CO_2 fixation (**d**) simulted under 550 μmol mol^{-1} CO_2 for all CO_2 × irrigation on 5 April 1994 (days 95)

SE of the measured values after mid-February except when leaf senescence under suboptimum irrigation was underestimated during April (Fig. 7a). The leaf area index in the model was increased under 550 μmol mol^{-1} CO_2 to 1.10 and 1.16 of its value under 355 μmol mol^{-1} CO_2 with optimum and suboptimum irrigation respectively. The value in the FACE experiment was no higher under 550 than under 355 μmol mol^{-1} CO_2 and optimum irrigation, but was increased by 1.23 with suboptimum irrigation before anthesis. The seasonal time course of phytomass growth was simulated within the SE of the measured values except when late-season growth under suboptimum irrigation was underestimated (Fig. 7b). Total phytomass at both [CO_2] was overestimated with optimum irrigation and underestimated with suboptimum irrigation (Table 2), mostly because senescence during May was not accurately simulated (Fig. 7b). Seasonal phytomass simulated and measured under 550 μmol mol^{-1} CO_2 was 1.14 and 1.10 that under 355 μmol mol^{-1} CO_2 with optimum irrigation, and 1.28 and 1.18 that under 355 μmol mol^{-1} CO_2 with suboptimum irrigation. These increases in the model arise directly from those in leaf CO_2 fixation (Figs. 5d, 6d) scaled to canopy CO_2 fixation as affected by increases in [CO_2].

Seasonal water use was simulated within 1 SE of measured values for all CO_2 × irrigation treatments (Table 2).The measured values of evapotranspiration were calculated as irrigation + rainfall −change in soil water content (0–2.1 m) between 10 January and 28 May 1994. The simulated values were total surface water fluxes (soil + canopy) between the same dates. Measured values of phytomass were averages of those from 11, 18 and 25 May, and simulated values were the maxima during the growing season. The water use data were taken from Hunsaker et al. (1996).

Simulated and measured water use under 550 μmol mol^{-1} CO_2 was about 6% lower than that under 355 μmol mol^{-1} CO_2 with optimum irrigation, and about 2% lower than that under 355 mol mol^{-1} CO_2 with suboptimum irrigation. These decreases in the model arise directly from those in canopy latent heat flux (Fig. 4c) as affected by decreases in stomatal conductance over time.

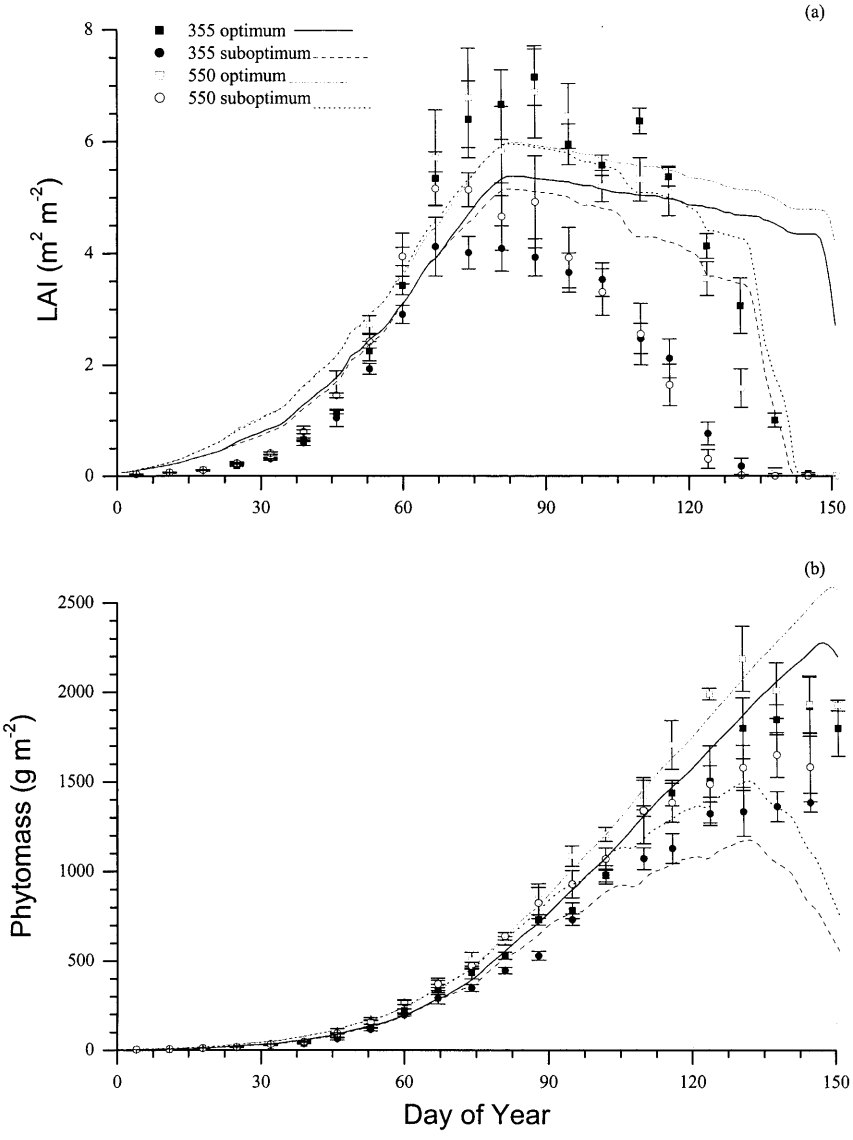

Fig. 7 **a** Leaf area index (*LAI*) **b** above-ground phytomass simulated (*lines*) and measured (*symbols*) under optimum or suboptimum water supply and 550 or 355 μmol mol^{-1} CO_2

Discussion

The soil–plant–atmosphere water-transfer scheme proposed above offers several advances in the simulation of land surface interactions:

First, the stomatal resistance model (Eq. 1) avoids assumptions in existing land surface schemes about interactions among environmental conditions (radiation, temperature, CO_2) upon stomatal behavior. These interactions are resolved in the calculation of CO_2 fixation (Eqs. 2 –7) in which processes are already well understood.

Second, the parameters of the model may be obtained from independent studies of stomatal response to CO_2 fixation conducted at temporal and spatial scales smaller than those at which the land surface scheme will predict (e.g. Table 1). It should be acknowledged, however, that important plant features such as osmotic adjustment, are not represented in the model. In the case of a wheat canopy the osmotic adjustments that might be associated with water stress have been reported to be about 0.5 MPa (Simmelsgaard 1976). Although during water stress the osmotic adjustment can weaken the relationship between the leaf potential and the stomatal conductance, the value reported by Simmelsgaard (1976) was measured when the stomatal conductance tended to be close to zero. Therefore, although this model might be inaccurate under extremely severe water stress it is unlikely that field farming practices would allow a crop with economic value to experience such a level of stress. This supports the use of this model in land and water resource studies, while it does not support its use to investigate the physiological response of plant canopies under extremely water-limited conditions. Furthermore the risk of inaccuracy can become quite significant if we attempt to simulate mass and energy fluxes from a plant canopy such as cotton, in which an osmotic adjustment equal to 1.2 MPa has been reported, when the stomatal conductance tended to zero (Brown et al. 1976).

The model may be tested with a diverse set of routinely measured data (e.g. leaf conductance, water potential, CO_2 fixation, temperature) at spatial scales smaller than those at which the land surface scheme will predict (e.g. Figs. 5, 6).

Changes in leaf area index and root length are driven from internal C transfer processes that are sensitive to soil and climate constraints, providing opportunities to simulate more complex atmosphere–ecosystem interactions than is possible with models in whlch leaf area index and water uptake are prescribed.

In the proposed transfer scheme, stomatal conductance varies inversely with atmospheric [CO_2] and directly with leaf CO_2 fixation rate. The model thus reproduces the observation of Wong et al. (1979) that stomatal conductance varies with CO_2 fixation rate to maintain a constant CO_2 concentration ratio across the stomata. The responses of CO_2 fixation to 550 and 355 μmol mol^{-1} CO_2 were consistent with those measured in the FACE experiment at both diurnal (Figs. 5d, 6d) and seasonal (Fig, 7b) time scales. Because the internal [CO_2] is maintained as a constant fraction of the atmospheric [CO_2], carbon fixation increases with [CO_2] (Eq. 3): however, this increase in assimilation rate is not sufficient to compensate for the reduction in stomatal conductance caused by higher atmospheric [CO_2] (Eq. 1). Therefore the stomatal conductance in the model was lower under 550 than under 355 μmol mol^{-1} CO_2 to an extent that was consistent with reductions measured in the FACE experiment (Fig. 5b) and elsewhere (e.g. Morison 1985). Consequent reductions in latent heat flux (Fig. 4c, Table 2) and increases in canopy temperature (Figs. 5c, 6c) were also measured in the FACE experiment and elsewhere (Idso et al. 1987; Kimball et al. 1992b, 1995). Lower transpiration under 550 than under 355 μmol mol^{-1} CO_2 caused less-negative leaf water potential values (Figs. 5a), which were also measured in the FACE experiment and (Allen et al. 1994; Huber et al. 1984; Sionit et al. 1980).

Suboptimal by comparison with optimal irrigation caused lower soil water potential and hence lower leaf water potential (Fig. 5a), lower stomatal conductance (Fig. 5b), lower CO_2 fixation (Fig. 5d, Table 2) and higher canopy temperature (Fig. 5c). A less-negative leaf water potential under 550 than under 355 μmol mol^{-1} CO_2 caused stomatal resistance to rise less from unconstrained values during convergence to low water potentials, so that stomatal conductance was less affected by CO_2 under suboptimum than under optimum Irrigation (Fig. 5b). This reduced effect was apparent in both simulated and measured seasonal water use (Table 2). The significance of the $CO_2 \times$ irrigation interaction upon stomatal conductance was obscured by spatial variability in the measured values. However, both simulated and measured canopy temperatures increased less under 550 and 355 μmol mol^{-1} CO_2 with suboptimum than with optimum irrigation (Figs. 5c). The simulated $CO_2 \times$ irrigation interaction on stomatal conductance provides a mechanistic explanation for the observation of Allen et al. (1994) that conductance is little affected by CO_2 in water-stressed for the observation by Curtis (1996), Huber et al. (1984) and Rogers et al. (1984) that conductance decreases less with water stress under elevated than under ambient CO_2.

The smaller effect of CO_2 on stomatal conductance with suboptimum rather than, optimum irrigation in the model allowed a larger effect of CO_2 on CO_2 fixation with suboptimum than with optimum irrigation to be simulated at both the hourly (Fig. 5d) and seasonal (Fig. 7b, Table 2 time scales. This larger effect is consistent with findings from the FACE experiment (Table 2, Kimball et al. 1995) and elsewhere (Gifford 1979; Rogers et al. 1986) that plant growth increases more with CO_2 under water-limited conditions. These findings suggest that the effect of increased CO_2 on canopy mass and energy exchange depends upon soil water availability. Such dependence is an important terrestrial feedback to the atmosphere under gradually increasing atmospheric concentrations of CO_2.

Further work is needed to refine some of the model algorithms. The underestimation of phytomass in the suboptimum irrigation treatment may have been caused by the assumption that the constraint imposed by stomatal resistance on CO_2 fixation is commensurate with that Imposed on transpiration whereas it can be slightly less. The underestimation may also have been caused by the requirement in the model that all irrigations be applied at the canopy surface whereas the FACE irrigations were applied below the soil surface, thereby reducing unproductive evaporation. The overestimation of the leaf area index in the suboptimum irrigation treatment will require reconsideration of the algorithm for leaf senescence. There is also a need for further development of the algorithm for root extension because it controls the rate at which soil water reserves are accessed by the plant canopy.

References

Allen LH Jr, Valle RR, Mishoe JW, Jones JW (1994) Soybean leaf gas-exchange responses to carbon dioxide and water stress. Agron J 86:625-636

Amthor JS (1984) The role of maintenance respiration in plant growth. Plant Cell Environ 7:561-569

Ball JT (1987) Calculations related to gas-exchange. In: Ziegler G, Farquhar GD, Cowan I R (eds) Stomatal function. Stanford University Press, calif pp 445-476

Ball JT (1988) An analysis of stomatal conductance. PhD Thesis, Stanford University, calif, p 89

Brown KW, Jordan WR, Thomas JC (1976) Water stress induced alterations of the stomatal response to decreases in leaf water potential. Physiol Plant 37:1-5

Campbell GS (1985) Soil physics with basic. Transport models for soil plant systems. Dev Soil Sci 14:122-129

Chaves MM (1991) Effects of water deficits on carbon assimilation. J Exp Bot 42:l-16

Clapp RB, Hornberger GM (1978) Empirical equations for some soil hydraulic properties. Water Resour Res 14:601-604

Cline RG, Campbell GS (1976) Seasonal and diurnal water relations of selected forest species. Ecology 57:367-373

Collatz G, Ball JT, Grivet C, Berry JA (1991) Physiological and environmental regulation of stomatal conductance, photosynthesis and transpiration: a model that includes a laminar boundary layer. Agric For Meteorol 54:107-136

Cowan IR (1965) Transport of water in the soil–plant– atmosphere system. J Appl Ecol 2:221-239

Curtis PS (1996) A meta-analysis of leaf gas exchange and nitrogen in trees grown under elevated carbon dioxide. Plant Cell Environ l9:127-137

Douglas BJ, Ogren WL (1984) The CO_2 /O_2 specificity of ribulose 1,5-biphosphate carboxylase/oxygenase. Planta 161:308-313

Evans JR, Farquhar GD (I991) Modelling canopy photosynthesis from the biochemistry of the C_3 chloroplast. In: KJ Boote, RS Loomis (eds) Modeling crop photosynthesis from biochemistry to canopy. CSSA Spec publ. 19:1-15

Farquhar GD, Caemmerer S von (1982) Modelling of photosynthetic response to environment. In: Lange OL, Nobel PS, Osmond CB, Ziegler H (eds) Encyclopedia of plant physiology. (New series vol 12B. Physiological plant Ecology II) Springer Berlin Heidelberg New York, pp 549-587

Farquhar GD, Caemmerer S von, Berry JA (1980) A biochemical model of photosynthetic CO_2 assimilation in leaves of C_3 species. Planta 149:78-90

Foley JA (1995) Numerical models of the terrestrial biosphere. J Biogeogr 22:837-842

Foley JA, Colin P, Ramankutty N, Levis S, Pollard D, Sitch S, Haxeltine A (1996) An integrated biosphere model of land surface processes, terrestrial carbon balance, and vegetation dynamics. Glob Biogeochem Cycles 10:603-628

Forseth IN, Norman JM (1993) Modelling of solar irradiance, leaf energy budget and canopy photosynthesis. In: Hall DO, Scurlock JMO, Bulhar H, Leegood RC, Long SP (eds) Photosynthesis and production in changing environment: a field and laboratory manual. Chapman and Hall, London, pp 207-219

Gardner WR (1960) Dynamics aspects of water availability to plants. Soil Sci 89:63-73

Garratt JR (1993) Sensitivity of climate simulations to land-surface and atmospheric boundary-layer treatments—a review. J Climate 6:419-449

Gifford RM (1979) Growth and yield of CO_2 -enriched wheat under water-limited conditions. Aust J Plant Physiol 6:367-378

Glatzel G (1983) Mineral nutrition and water relations of hemiparasitic mistletoes: a question of partitioning. Experiments with *Loranthus europaeus* on *Quercus petrea* and *Quercus robur*. Oecologia 56:193-201

Grant RF (1989) Test of a simple biochemical model for photosynthesis of maize and soybean leaves. Agric For Meteorol 48:59-74

Grant RF, Wall GW, Kimball BA, Frumau KFA, Pinter, PJJr, Hunsaker DJ, Lamorte RL (1999) Crop water relations under different CO_2 and irrigation: testing of *ecosys* with the free. air enrichment (FACE) experiment. Agric For Meteorol 95:27-51

Guehl JM, Picon C, Aussenac G Gross P (1994) Interactive effects of elevated CO_2 and soil drought on growth and transpiration efficiency and its determinants in two European forest tree species. Tree Physiol 14:707-724

Huber SC, Rogers HH, Mowry FL (1984) Effects of water stress on photosynthesis and carbon partitioning in soybean *(Glycine Max*. [L.] Merr.) plants grown in the field at different CO_2 levels. Plant Physiol 76:244-249

Hunsaker DJ, Kimball BA, Pinter JP Jr, LaMorte RL, Wall GW (1996) Carbon dioxide enrichment and irrigation effects on wheat evapotranspiration and water use efficiency. Trans ASAE 39:1345-1355

Idso SB, Kimball BA, Mauney JR (1987) Atmospheric carbon dioxide enrichment effects on cotton midday foliage temperature: implications for plant water use and crop yield. Agron J 79:667-672

Jarvis PG (1976) The interpretation of the variation in leaf water potential and stomatal conductance found in canopies in the field. Philos Trans R Soc London [Biol] 273:593-610

Jones HG, Higgs KH (1989) Empirical models of the conductance of leaves in apple orchards. Plant Cell Environ 12:301-308

Keulen H van, Selingman NG (1987) Simulation of water use, nitrogen nutrition and growth of a spring wheat crop. Simulation Monographs Pudoc, Wageningen, pp 18-89

Kimball BA, Idso SB (1983) Increasing atmospheric CO_2: effects on crop yield, water use and climate. Agric Water Manage 7:55-72

Kimball BA, LaMorte RL, Peresta GJ, Mauney JR, Lewin KF, Hendrey GR (1992a) Appendix 1. Weather, soils, cultural practices, and cotton growth data from the 1989 FACE experiment in IBSNAT format. Crit Rev Plant Sci 11:271-308

Kimball BA, Pinter RL PJ Jr, Mauney JR (1992b) Cotton leaf and boll temperatures in the 1989 FACE experiment. Crit Rev Plant Sci 11:233-240

Kimball BA, Pinter JP Jr, Garcia RL, LaMorte RL, Wall GW, Hunsaker D, Wechsung G, Wechsung F, Kartschall T (1995) Productivity and water use of wheat under free-air CO_2 enrichment. Global Change Biol 1:429-442

Lewin KF, Hendrey GR, Nagy J, LaMorte R (1994) Design and performance of a free-air carbon dioxide enrichment facility. Agric For Meteorol 70:15-30

Mahrt L, Ek M (1984) The influence of atmospheric stability on potential evaporation. J Clim Appl Meteorl 23:222-234

McCree KJ (1988) Sensitivity of sorghum grain yield to ontogenetic changes in respiration coefficients. Crop Sci 28:114-120

Miglietta F, Giuntoli A, Bindi M (1996) The effect of free-air carbon dioxide enrichment (FACE) and soil-nitrogen availability on the photosynthetic capacity of wheat. Photosynthesis Res 47:281-290

Morison JIL (1985) Sensitivity of stomata and water use efficiency to high CO_2. Plant Cell Environ 8:467-474

Norman JM (1993) Scaling processes between leaf and canopy 1evels. In: Ehleringer JR, Field CB (eds) Scaling physiological processes: leaf to globe. Academic Press, San Diego, calif, pp 41-79

Passioura JB, Cowan IR (1968) On solving the non-linear diffusion equation for the radial flow of water to the roots. Agric Meteorol 5:129-134

Prentice IC, Cramer W, Harrison SP, Leemans R, Monserud RA, Solomon AM (1992) A global biome model based on plant physiology and dominance, soil properties and climate. J Biogeogr 19:117-134

Pinter PJJr, Kimball BA, Garcia RL, Wall GW, Hunsaker DJ, LaMorte RL (1996) Free-Air CO_2 enrichment: responses of cotton and wheat crops. In: Koch GW, Mooney HA (eds) Carbon dioxide and terrestrial ecosystems. Academic Press, San Diego, calif, pp 215-249

Raschke K (1979) Movements using turgor mechanism. In: Haupt W, Feinlieb ME (eds) Encyclopedia of plant physiology. (New series, vol 7, Physiology of movement) springer, Berlin Heidelberg New York, pp 383-434

Rogers HH, Sionit N, Cure JD, Smith JM, Bingham GE (1984) Influence of elevated carbon dioxide on water relations of soybeans. Plant Physiol 74:933-238

Rogers HH, Cure JD, Smith JM (1986) Soybean growth and yield response to elevated carbon dioxide. Agric Ecosyst Environ l6:113-128

Sellers PJ, Randall DA, Collatz GJ, Berry JA, Field CB, Dazlich DA, Zhang C, Collelo GD, Bounoua L (1996) A revised land surface parameterization (SiB2) for atmospheric GCMs. Part I: model formulation. J Climate 9:676-705

Senock RS, Ham JM, Loughin TM, Kimball BA, Hunsaker DJ, Pinter PJJr, Wall GW, Garcia RL, LaMorte RL (1996) Sap flow in wheat under free-air CO_2 enrichment. Plant Cell Environ 19:147-158

Sharpe PSH, De Michelle DW (1977) Reaction kinetics of poikilothermic development. J Theor Biol 64:249-670

Sicher RC, Bunce JA (1997) Relationship of photosynthetic acclimation to changes in Rubisco activity in field grown winter wheat and barley during growth in elevated carbon dioxide. Photosynthesis Res 52:27-38

Simmelsgaard SE (1976) Adaptation to water stress in wheat. Physiol Plant 37:167-174

Sionit N, Hellmers H, Strain BR (1980) Growth yield of wheat under CO_2 enrichment and water stress. Crop Sci 20:687-690

Steward JB (1988) Modelling surface conductance of pine forests. Agric For Meteorol 43:19-35

Van Bavel CHM, Hillel D1 (1976) Calculating potential and actual evaporation from a bare soil surface by simulation of concurrent flow of water and heat. Agric Meteorol 17:456-476

Verseghy DL (1991) CLASS—a Canadian land surface scheme for GCMS. I. Soil model. Int J Climato1 11:111-113

Verseghy DL, McFarlane, NA, Lazare, M (1993) CLASS – A Canadian land surface scheme for GCMS. II. Vegetation model and coupled runs. Int J Climatol 13:347-370

Wilhelm E, Battino R, Wilcock RJ (1977) Low-pressure solubility of gases in liquid water. Chem Rev 77:219-262

Williams K, Caldwell MM, Richards JH (1993) The influence of shade and clouds on soil water potential: the buffered behavior of hydraulic lift. Plant Soil 157:83-95

Wong SC, Cowan IR, Farquhar GD (1979) Stomatal conductance correlates with photosynthetic capacity. Nature 282:424-426